Egyptian Journal of Petroleum (2011) **20**, 47–57

Egyptian Petroleum Research Institute

Egyptian Journal of Petroleum

www.elsevier.com/locate/egyjp
www.sciencedirect.com

Novel cationic surfactants from fatty acids and their corrosion inhibition efficiency for carbon steel pipelines in 1 M HCl

A.M. Al-Sabagh [a,*], N.Gh. Kandil [b], O. Ramadan [b], N.M. Amer [a], R. Mansour [a], E.A. Khamis [a]

[a] *Department of Petroleum Applications, Egyptian Petroleum Research Institute (EPRI), Ahmed El-Zomor Street 1, Nasr City, Cairo 11727, Egypt*
[b] *Chemistry Department, Faculty of Girls for Science, Art and Education, Ain Shams University, Asmaa Fahmi Street, Helliopolis, Cairo, Egypt*

Available online 5 October 2011

KEYWORDS

Cationic surfactant;
Quaternary ammonium salts;
Weight loss;
Potentiodynamic and quantum chemical calculations

Abstract Four fatty acids were used as a source of alkyl halides. Untraditionally tertiary amines were prepared by ethoxylation of aromatic and aliphatic fatty amines. These alkyl halide and tertiary amines were used to prepare 20 cationic quaternary ammonium surfactants (QAS_S). Their chemical structures were characterized and they tested as corrosion inhibitors for carbon steel in 1 M HCl solution. The corrosion inhibition efficiency was measured using, weight loss and potentiodynamic polarization methods. The inhibition efficiencies obtained from the two employed methods are nearly closed. From the obtained data it was found that, the inhibition efficiency increases with increasing the inhibitor concentration until the optimum one. Also, it was found that the inhibition efficiency of QASs which based on ethoxylated aromatic tertiary amine is greater than the obtained efficiencies by the QASs which based on ethoxylated aliphatic tertiary amines. The QASs based on alkyl halide C16 exhibited the maximum inhibition efficiency 98.8%. Adsorption of the inhibitors on the carbon steel surface was found to obey Langmuir's adsorption isotherm. The quantum chemical calculations were done for some selected quaternary ammonium compounds based on their chemical structures QL1,4,5–QP3,4,5. The following quantum chemical indices such

* Corresponding author.
E-mail address: alsabaghh@gmail.com (A.M. Al-Sabagh).

Peer review under responsibility of Egyptian Petroleum Research Institute.
doi:10.1016/j.ejpe.2011.06.007

Production and hosting by Elsevier

as the bond length, bond angle, charge density distribution, highest occupied molecular orbital (HOMO), lowest unoccupied molecular orbital (LUMO), energy gap ΔE = HOMO – LUMO, and dipole moment (u) were considered. The relation between these parameters and the inhibition efficiencies was explained on the light of the chemical structure of the used inhibitors.

1. Introduction

The use of organic inhibitors is one of the most practical methods for protection against corrosion in acidic media [1]. The choice of the inhibitor is based on two considerations: first it could be synthesized conveniently from relatively cheap raw materials, secondly, it contains the electron cloud on the aromatic ring or, the electronegative atoms such as nitrogen and oxygen in the relatively long chain compounds [2]. Due to the presence of the ─C═N group in the cationic surfactant, they should be good corrosion inhibitors. Among all inhibitors, the most important are the organic ones, also called adsorption inhibitors [3]. They control corrosion, acting over the anodic or the cathodic surface or both. Most commercial acid inhibitors are organic compounds containing heteroatoms such as nitrogen, oxygen, sulfur, phosphor atoms, by which the inhibitor molecules are adsorbed on the metal surface in acidic media [4–9]. Thus resulting adsorption film by surfactants acts as a barrier separating the metal from the corrosive medium and blocks the active sites. As a representative type of these organic inhibitors, quaternary ammonium salts have been demonstrated to be highly cost-effective and used widely in various industrial processing for preventing corrosion of iron and steel in acidic media .The inhibition of steel corrosion has been achieved by many workers [10–20].

The objective of this work is to prepare some quaternary ammonium salts (QASs) based on untraditional tertiary amines. Free fatty acids lauric acid, palm acid, myristic acid and olic acid reduced to obtain fatty alcohols. The prepared fatty alcohols reacted with hydrobromic acid to obtain the corresponding alkyl halides. Aliphatic and aromatic amines ethoxylated (2 e.o.) to prepare untraditional tertiary amine. The QASs will be prepared by refluxing alkyl halide with the 3° amine. Our attention could be extended to characterize these products and testing them as corrosion inhibitors in 1 M HCl.

2. Experimental methods and materials

2.1. Preparation of fatty alcohols and alkyl halides

The fatty acids namely, lauric acid, palm acid, myristic acid and olic acid were reduced as described elsewhere [21]. The prepared fatty alcohols reacted with hydrobromic acid to form the corresponding alkyl fatty halides.

2.2. Preparation of 3° amine

Aromatic amine (aniline) and different aliphatic amines were charged individually into the reaction vessel without catalyst and heated with continuous stirring while passing a stream of nitrogen gas through the system for 10 min at 80 °C. The nitrogen stream was then replaced by ethylene oxide (2 mol) gas at a rate which was regulated by monitoring the Hg level of the manometer [22].

2.3. Preparation of quaternary ammonium salts

The prepared ethoxylated amines with alkyl halide in the molar ratio 1:1 were allowed to reflux in acetone for 12 h to obtain 20 QASs. The produced compounds were recrystallized twice from acetone with diethyl ether. The products were kept in desiccators up to use them [23]. Fig. 1 shows the general formula and designation of the prepared QASs. The chemical structure of the synthesized compounds was characterized by FTIR and ^{1}H NMR spectroscopic analysis.

2.4. Corrosion inhibition test

The aggressive solution, 1 M HCl, was prepared by dilution of analytical grade 37% HCl with distilled water. The concentration range of the prepared cationic surfactants was from 25 to 400 ppm used for corrosion measurements. All solutions were prepared using distilled water.

2.5. Weight loss technique

The specimens with dimensions 3 cm × 7.5 cm × 0.5 cm were used. The chemical composition of the specimens were:

C	Mn	P	Si	S	Cr	Mo	Fe
0.17	1.18	0.008	0.27	0.008	0.27	0.04	Rest

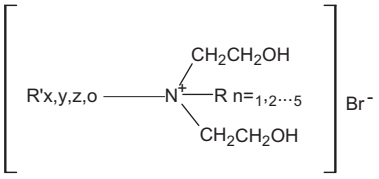

where

R'$_x$= (Lauric acid) namely QL$_{n1\text{-}5}$

R'$_y$ = (Palm acid) namely QP$_{n1\text{-}5}$

R'z= (Myristic acid) namely QM$_{n1\text{-}5}$

R'o=(Oleic acid) namely QO$_{n1\text{-}5}$

R$_{1\text{-}5}$ =3° amine from ethoxylated aliphatic and aromatic amine

Where n, 1= dodecylamine e.o,2

2=tetradecyl amine e.o,2

3= hexadecyl amine e.o,2

4=Triethyl amine

5= aniline e.o,2

Figure 1 The general formula of the prepared quaternary ammonium salts.

The samples were allowed to stand for 48 h in 1 M HCl solution in the absence and presence of different concentrations of the inhibitors.

2.6. Electrochemical technique

For electrochemical measurements, a conventional three-electrode glass cell with a platinum counter-electrode and a saturated calomel electrode (SCE) as a reference was used. Carbon steel rod of the same composition as working electrode was pressure fitted into a polytetrafluoroethylene (PTFE) holder exposing only a 0.7 cm^2 surface to the solution. The exposure surface was abraded with different grades of emery paper, degreased with acetone [24], washed with bidistilled water and finally dried. The experiments were carried out at constant temperature (within ± 1 °C).

2.7. Quantum chemical study

The molecular structures of the QASs had been fully geometric optimize by ab initio method (3-21G** basis set) with Hyperchem 7.5, the following quantum chemical indices such as the bond length, bond angle, charge density distribution, highest occupied molecular orbital (HOMO), lowest unoccupied molecular orbital (LUMO), energy gap ΔE = HOMO − LUMO and dipole moment (u) were considered.

3. Results and discussion

3.1. Confirmation of chemical structure of the prepared inhibitors

The chemical structure of the prepared cationic surfactants was confirmed by the FTIR and ^{1}H NMR spectroscopy for QP3 as representative sample. From the obtained spectra, it was found that the main band denotes to N^+ appeared at 1351 cm^{-1}. The C–O band of the ethoxylated $C_{16}H_{33}NH_2$ (primary amine) appeared at 1120 cm^{-1}. The terminal –OH group of ethoxylated primary amine was found at 3380 cm^{-1} as a broad band. The ^{1}H NMR of the same inhibitor, showed that, the main characteristic splitting band of –O$\underline{H}$ (from ethoxylated 3° amine) was found at chemical shift 3.57, C$\underline{H_3}$ δ, 0.82, C$\underline{H_2}$ δ, 1.2. The FTIR and ^{1}H NMR together confirmed the chemical structure of the prepared compound.

3.2. Weight loss measurements

The inhibition efficiency I.E.% was determined by the equation:

$$\text{I.E.}\% = \frac{\Delta W - \Delta W_i}{\Delta W} \times 100 \quad (1)$$

where ΔW and ΔW_i are the weight loss per unit area in absence and presence of inhibitor, respectively. Fig. 2 shows the inhibition efficiency against concentration for QL_n and QP_n as representative sample for the lowest and highest I.E., it can be observed that I.E. increases with increasing inhibitor concentrations.

Through studying the effect of inhibition efficiency, the rate of corrosion (CR) was calculated by the following equation [25]:

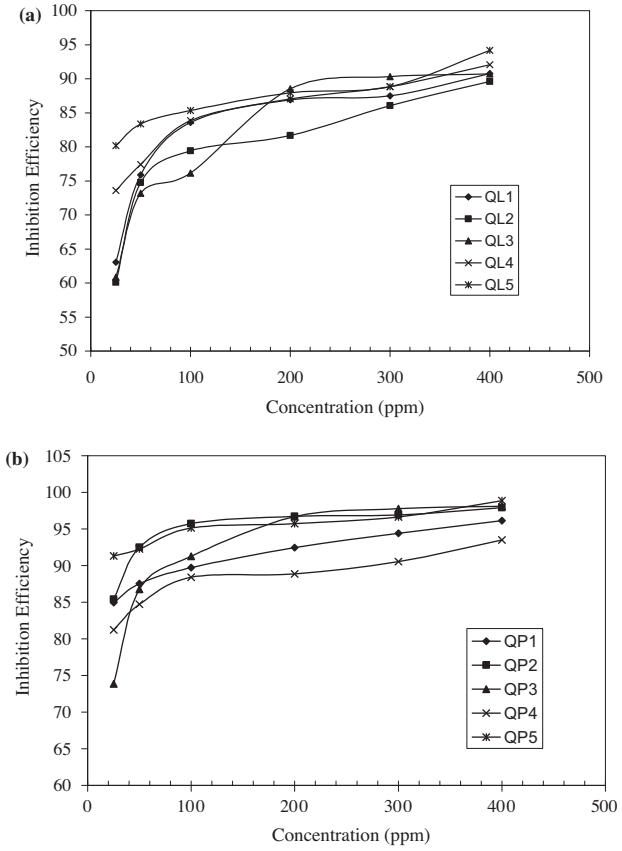

Figure 2 Inhibition efficiency against the concentrations of (a) QL_n and (b) QP_n for carbon steel dissolution in 1 M HCl.

$$\text{CR} = \Delta \frac{W \times 3.45 \times 10^{-6}}{A \times t \times D} \quad (2)$$

where ΔW is the mass loss in gram, A is the area in cm^2, t is the time in hours and D is the density in g/cm^3.

Fig. 3 illustrates the relation between the rates of corrosion against the inhibitor concentrations. The data obtained for corrosion rate (in mpy) for QL_n and QP_n as representative sample in presence of 200 ppm at 308 K are shown in Tables 1 and 2. The data show that the rate of corrosion for the blank sample is the highest one.

On the other hand, the surface coverage area (θ) for the different concentrations of the investigated inhibitors in 1 M HCl was calculated by the following equation:

$$\theta = 1 - (\Delta W_i / W_0) \quad (3)$$

The obtained data for θ are summarized in Tables 1 and 2. It is recognizable that, there is an inverse relation between the rate of corrosion and the surface coverage area. In other words, the inhibitors having higher surface coverage area are those having higher inhibition efficiency and lower corrosion rate. It was found that, the inhibition efficiency of QL which based on ethoxylated aromatic 3° amine is greater than that obtained by the QL which based on ethoxylated aliphatic 3° amine. The values of θ are in the range of ≈0.92 and ≈0.88, respectively. Also, is the inhibition efficiency of QP which based on ethoxylated aromatic 3° amine also, greater than that

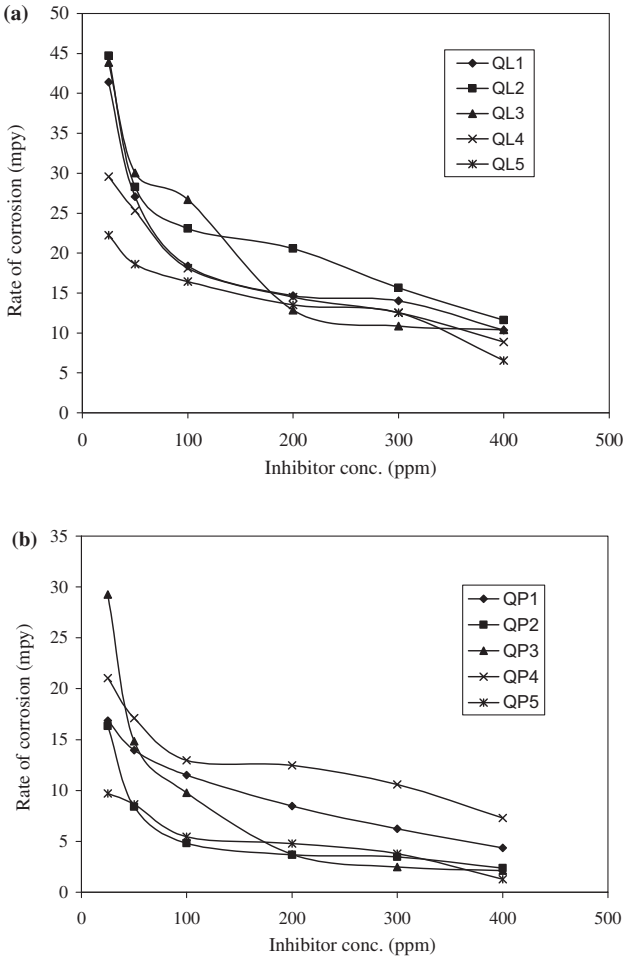

Figure 3 Rate of corrosion for carbon steel dissolution in 1 M HCl at different concentrations of the Inhibitor (a) QL_n and (b) QP_n.

obtained by the QP which based on ethoxylated aliphatic 3° amine. Their θ values are in the range of ≈0.98 and ≈0.96, respectively.

The inhibition efficiency of inhibitors was ranked as follows: $QP_n > QO_n > QM_n > QL_n$.

The high θ value near unity indicates almost a full coverage of the metal surface with adsorbed surfactant molecules. Conclusively, the surfactant inhibitor having θ near unity, is considered as a good physical barrier shielding the corroding surface from corrosive medium and dumping the corrosion rate of carbon steel significantly.

3.3. Effect of inhibitor concentration

The inhibiting effect increased with the increase of surfactant concentration as shown in Fig. 2 Hence, the corrosion rate was a concentration dependent. At low surfactant concentrations the adsorption takes place by binding to hydrophobic region as seen in Sketch 1. In other words, a mono disordered layer may be formed. This adsorption was a competitive one because the inhibitor displaces progressively the water molecules and other ions adsorb on the metal surface. When surfactant concentration increases, un-complete packing layer of the inhibitor molecules was formed in which adsorption takes

Table 1 Corrosion rate and degree of surface coverage (θ) at different concentrations of QL_n in 1 M HCl solution at 298 K. Using weight loss measurements.

Inhibitors code	Concentration (ppm)	Rate of corrosion (mpy)	(θ)
Blank	–	112.01	–
QL1	25	41.39	0.63
	50	27.04	0.75
	100	18.36	0.83
	200	12.68	0.88
	300	14.02	0.89
	400	9.34	0.91
QL2	25	44.70	0.60
	50	28.25	0.74
	100	23.06	0.79
	200	20.55	0.81
	300	15.63	0.86
	400	11.62	0.89
QL3	25	43.86	0.60
	50	30.05	0.73
	100	26.70	0.76
	200	16.84	0.86
	300	10.84	0.90
	400	10.38	0.90
QL4	25	29.56	0.73
	50	25.31	0.77
	100	18.09	0.83
	200	14.48	0.87
	300	12.51	0.88
	400	11.88	0.89
QL5	25	22.22	0.80
	50	18.63	0.83
	100	16.42	0.85
	200	8.15	0.92
	300	7.51	0.93
	400	6.54	0.94

place as a result of an inter-hydrophobic chain interactions which clear in Sketch 2. In other words, the increase in inhibition efficiency observed at higher inhibitor concentrations indicates that more inhibitor molecules were adsorbed on the metal surface, thus providing wider surface coverage [26]. Meanwhile at the over dose concentration (at maximum inhibition efficiency obtained), the inter space area between the adsorbed inhibitor molecules on the surface may be lesser than the area of the inhibitor molecules. So that, the inhibitor molecules turn out to form the double layer adsorption as shown in Sketch 10 [27].

It can be inferred from the data shown in Fig. 2 that, the inhibition efficiency becomes nearly constant starting from 400 ppm. This concentration will be used as the up limit through this study. The highest value of surface coverage, "θ" near unity indicates almost a full coverage of the metal surface with the adsorbed surfactant.

3.4. Effect of temperature and chemical structure on I.E.

The effect of temperature on the inhibition efficiency for carbon steel in 1 M HCl solution in the absence and presence of 200 ppm of inhibitors at temperature ranging from 308 to

Table 2 Corrosion rate, degree of surface coverage (θ), at different concentrations of QP_n in 1 M HCl solution at 298 K. Using weight loss measurements.

Inhibitors code	Concentration (ppm)	Rate of corrosion (mpy)	(θ)
Blank	–	112.01	–
QP1	25	16.86	0.84
	50	13.94	0.87
	100	11.52	0.89
	200	8.47	0.92
	300	6.24	0.94
	400	4.34	0.96
QP2	25	16.32	0.854
	50	8.41	0.924
	100	5.80	0.947
	200	4.68	0.951
	300	4.47	0.955
	400	3.35	0.967
QP3	25	29.27	0.738
	50	14.83	0.867
	100	9.78	0.912
	200	1.37	0.967
	300	0.54	0.974
	400	0.45	0.976
QP4	25	21.02	0.812
	50	17.10	0.847
	100	12.97	0.884
	200	12.48	0.888
	300	10.58	0.905
	400	7.30	0.934
QP5	25	9.71	0.913
	50	8.63	0.922
	100	5.45	0.951
	200	4.72	0.977
	300	3.77	0.981
	400	1.29	0.988

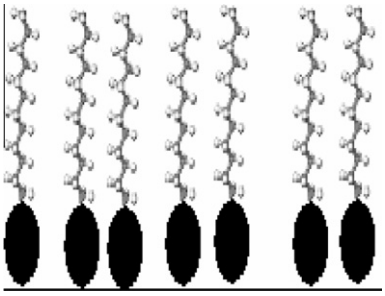

Sketch 1 The adsorption of inhibitor on the surface at low concentrations.

338 K was obtained in Tables 3 and 4. The inhibition efficiencies are found to decrease with increasing the solution temperature from 308 to 338 K. This behavior can be interpreted on the basis that the increase in temperature results in the desorption of the inhibitors from the surface of carbon steel [28].

A new relation was introduced to give the light on the relation between the inhibitor efficiency and the change of temperature along both series. The increment of decreased efficiency

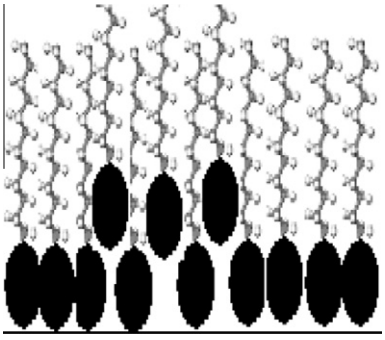

Sketch 2 The adsorption of inhibitor on the surface at high concentrations

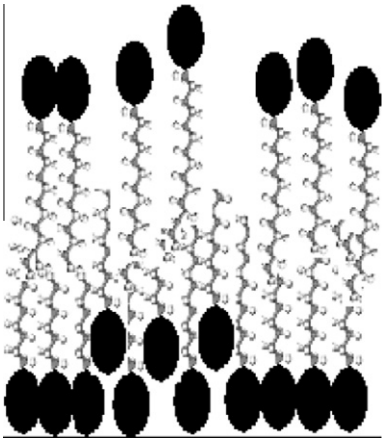

Sketch 3 The adsorption of inhibitor on the surface at the maximum inhibition efficiency obtained (over dose concentration).

per unit temperature (ΔI.E. /Δ°C) was calculated from the following equation:

$$\Delta\text{I.E.}/\Delta^{\circ}\text{C} = (\text{I.E.}_{t_1} - \text{I.E.}_{t_2})/(t_2 - t_1)$$
$$= (\text{I.E.}_{\text{at } 30^{\circ}\text{C}} - \text{I.E.}_{\text{at } 60^{\circ}\text{C}})/(60 - 30) \quad (4)$$

The inhibition efficiency at both the lowest (308 K) and the highest studied temperatures (338 K) and (ΔI.E./Δ°C) were listed in Table 5.

The low value of (ΔI.E./Δ°C) denotes that, the inhibitor exhibits the maximum I.E. By analysis of this data it was found that in the series of QL_{1-5} as example, the inhibitor QL1 (C12/C12 alkyl halide/alkyl of aliphatic 3° amine) gave ΔI.E./Δ°C equal 0.87. Otherwise in the series of QP_{1-5}, the QP3 exhibited the lowest value of ΔI.E./Δ°C (0.78). This observation mean that the optimum geometrical shape of the inhibitor molecule on the surface obtained at which the identical carbon number in the two chain of the molecule (C12, C16 for alkyl halid, and C12, C16 from 3° amine). So, that they exhibited the best I.E. While the maximum I.E. was obtained by the (C16 alkyl halide /C16 3° amine) inhibitor QP3.

In general the ΔI.E./Δ°C of QL_5 and QP_5 (0.78 and 0.70, respectively). This means that the aromatic 3° amine in the inhibitor structure is more effective in the inhibition than the aliphatic 3° amine.

Table 3 Corrosion rate, degree of surface coverage (θ), the inhibition percentage (I.E.%) and activation energy at different temperatures in 1 M HCl solution in presence of 200 ppm of QAS inhibitors.

Inhibitors code	Temperature (K)	Corrosion rate (mpy)	(θ)	(I.E.%)	E_a^* (kJ mol^{-1})
Blank	303	111.99	–	–	9.46
	318	148.248	–	–	
	328	165.809	–	–	
	338	174.032	–	–	
QL1	303	12.68	0.88	88.88	38.06
	318	26.82	0.81	81.90	
	328	44.04	0.73	73.43	
	338	66.15	0.61	61.98	
QL2	303	20.55	0.81	81.64	26.68
	318	34.83	0.76	76.50	
	328	44.37	0.73	73.23	
	338	96.13	0.44	44.75	
QL3	303	16.84	0.86	86.52	30.04
	318	20.98	0.85	85.84	
	328	40.16	0.75	75.77	
	338	67.93	0.60	60.96	
QL4	303	14.48	0.87	87.06	28.68
	318	30.99	0.79	79.08	
	328	45.50	0.72	72.55	
	338	98.61	0.43	43.33	
QL5	303	8.15	0.92	92.31	33.43
	318	20.95	0.85	85.86	
	328	41.62	0.74	74.89	
	338	51.47	0.70	70.42	

Table 4 Corrosion rate, the degree of surface coverage (θ), the inhibition percentage (I.E.%) and activation energy at different temperatures in 1 M HCl solution in presence of 200 ppm of QAS inhibitors.

Inhibitors code	Temperature (K)	Corrosion rate (mpy)	(θ)	(I.E.%)	E_a^* (kJ mol^{-1})
Blank	303	111.99	–	–	9.46
	318	148.248	–	–	
	328	165.809	–	–	
	338	174.032	–	–	
QP1	303	8.47	0.92	92.43	44.63
	318	26.19	0.82	82.32	
	328	50.24	0.69	69.69	
	338	79.25	0.54	54.46	
QP2	303	4.68	0.95	95.10	60.54
	318	15.57	0.80	80.01	
	328	52.80	0.68	68.15	
	338	55.12	0.49	49.14	
QP3	303	1.37	0.96	96.72	68.77
	318	36.20	0.75	75.58	
	328	61.81	0.62	62.72	
	338	45.58	0.73	73.21	
QP4	303	12.48	0.88	88.85	36.17
	318	31.29	0.78	78.89	
	328	46.45	0.71	71.98	
	338	71.34	0.59	59.00	
QP5	303	4.72	0.97	97.73	47.68
	318	15.93	0.89	89.25	
	328	29.09	0.82	82.45	
	338	40.97	0.76	76.52	

3.5. Adsorption isotherm

As known that organic inhibitors establish their inhibition via the adsorption of the inhibitor molecules onto the metal surface. The adsorption process is influenced by the chemical structures of compound, the distribution of charge in molecule, the nature and surface charge of metal and the type of aggressive media [29].

The values of surface coverage for the different concentrations of the studied inhibitors have been used to explain the best adsorption isotherm to determine the adsorption process. The data obtained from different techniques have been tested with several adsorption isotherms. Langmuir adsorption isotherm was found to fit well with our experimental data. A straight line was obtained on plotting $\log \theta/(1-\theta)$ vs. $\log C$ (concentration of inhibitors) as shown in Fig. 4 which suggested that the adsorption of the inhibitors used from 1 M HCl solutions on carbon steel follows Langmuir's adsorption isotherm.

3.6. Thermodynamic parameters of corrosion

The values of activation energy (E_a) were calculated from Arrhenius equation [30]:

$$\log K = (E_a/2.303R) \cdot 1/T + A \text{ (constant)} \quad (5)$$

where $\log K$ is the corrosion rate of metal, A is the frequency factor, T is the absolute temperature and R is the universal gas constant.

Table 5 Inhibition Efficiency depression regarding to the Increase in temperature for the investigated inhibitors.

	Inhibition efficiency (I.E.%)		ΔI.E.	ΔI.E./Δ°C
	30 °C	60 °C		
QL1	88.28	68.12	26.3	0.876
QL2	81.64	54.46	36.89	1.229
QL3	86.52	61.98	25.56	0.852
QL4	87.06	43.33	43.73	1.457
QL5	92.31	70.42	21.89	0.729
QP1	92.43	44.75	38.03	1.267
QP2	95.1	49.14	45.96	1.532
QP3	96.72	73.21	23.51	0.783
QP4	88.85	59.00	29.85	0.995
QP5	97.73	76.52	21.21	0.707

Fig. 5 represents the plot of corrosion rate (K) vs ($1/T$) for carbon steel in 1 M HCl solution in the absence and presence of 200 ppm of compound QL_n, and QP_n. The straight lines were obtained with slope equal to $-E_a/R$. Values of E_a were calculated and recorded in Table 6. Inspection of Table 6 reveals that the values of activation energy obtained in presence of prepared cationic surfactant are smaller than that obtained in free acid solution [31]. This means that, carbon steel corrosion occurs at the uncovered part of the surface. Thus adsorption of inhibitors was assumed to occur on the higher energy sites. The presence of inhibitor compounds which result in

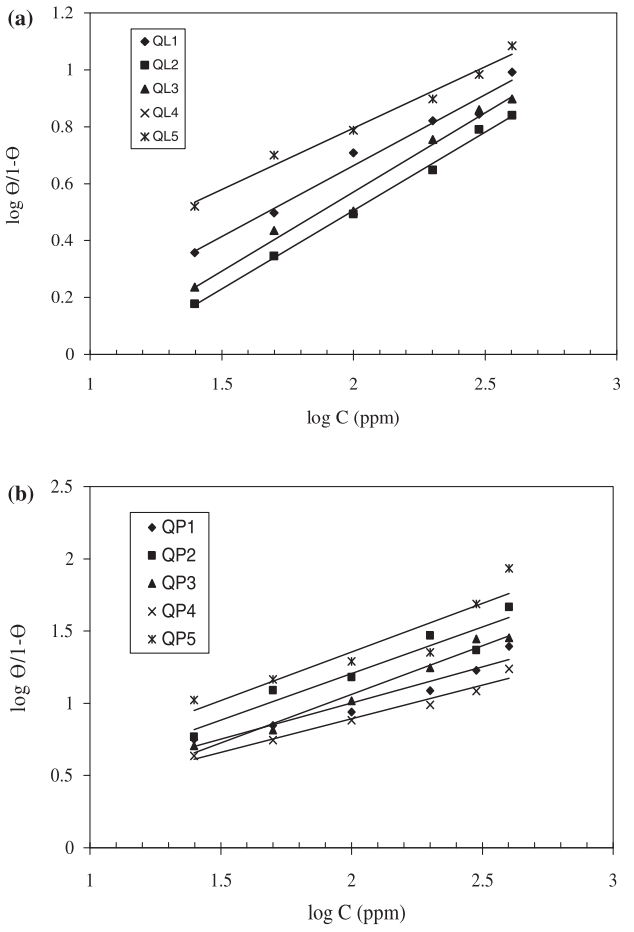

Figure 4 Langmuir adsorption isotherm of (a) QL_n and (b) QP_n for carbon steel in 1 M HCl solution.

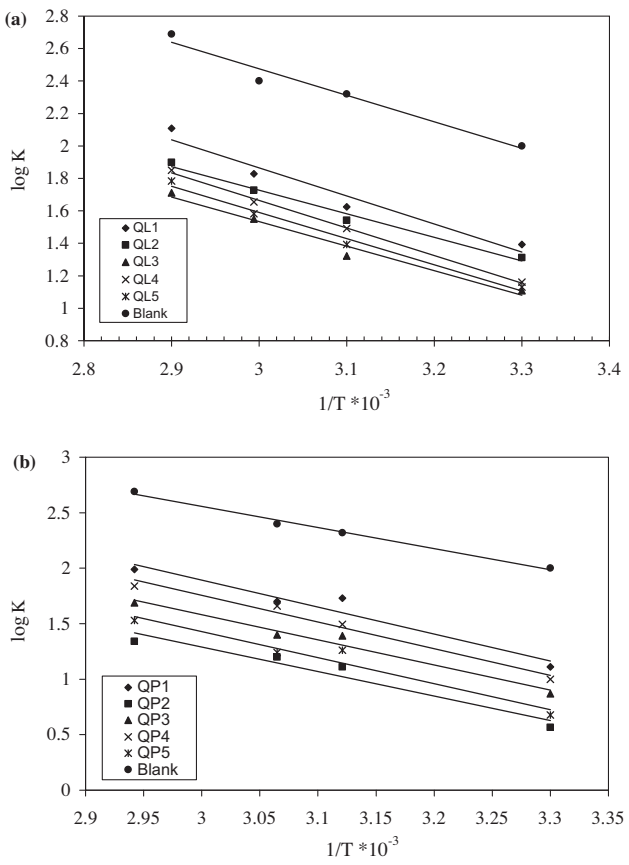

Figure 5 $\log K - 1/T$ curves for carbon steel dissolution in 1 M HCl in absence and presence of 200 ppm of inhibitors (a) QL_n and (b) QP_n at different temperatures.

the blocking of the active sites must be associated with an increase in the activation energy (E_a^*) of carbon steel in the inhibited sites.The free energy of activation (ΔG_{ads}^*) at different temperatures was calculated from the following equation [24,23–33]:

$$-\Delta G_{ads}^* = RT\ln(55.5\ k_{ads}) \tag{6}$$

$$k_{ads} = \theta/C_{inh}(1-\theta)$$

where k_{ads} is the equilibrium constant of the inhibitor adsorption process, the value 55.5 is the molar concentration of water in solution in mol dm^{-3}, R is the gas constant, T is absolute temperature and ΔG_{ads}^* is the standard free energy of adsorption.

The calculated values of the adsorption free energy, ΔG_{ads}^* and adsorption enthalpies, ΔH_{ads}^* are given in Table 6.

The calculated ΔG_{ads}^* values indicated that the adsorption mechanism of the prepared cationic surfactants on carbon steel in 1 M HCl solution is mixed physical and chemical adsorption [34]. The large values of ΔG_{ads}^* and its negative sign are usually characteristic of strong interaction and a highly efficient adsorption. The positive value of ΔH_{ads}^* indicated that adsorption of the investigated inhibitors on the carbon steel surface in 1 M HCl is endothermic.

The data show that the thermodynamic activation functions (E_a^* and ΔH_{ads}^*) of the corrosion of carbon steel in 1 M HCl solution in the presence of the inhibitors are higher than those in the free acid solution. E_a^* and ΔH_{ads}^* enhance with increasing inhibitor concentration, indicating more energy barrier for the reaction in the presence of the inhibitor is attained.Entropy of inhibition adsorption (ΔS_{ads}^*) was calculated using the following equation [35]:

$$\Delta G_{ads}^* = \Delta H_{ads}^* - T\,\Delta S_{ads}^* \tag{7}$$

It is clear that from Table 6 ΔS_{ads}^* values in the presence of the prepared cationic surfactants have positive sign, which mean that, an increase in ordering takes place in going from reactants to the M_{ads} reaction complex.

3.7. Potentiodynamic polarization curves

The potentiodynamic polarization curves for carbon steel in 1 M HCl solution with 200 ppm of inhibitors at 10 mV s^{-1} are shown in Fig. 6. Values of associated electrochemical parameters such as a corrosion potential E_{corr}, polarization resistance (R_P), corrosion current density (I_{corr}) and inhibition efficiency (I.E.%) for all the inhibitors were calculated and listed in Table 7. The percentage inhibition efficiency was calculated using the following equation [24,36,37]:

$$\text{I.E.\%} = [(I_{corr} - I_{corr}(\text{inh})/I_{corr})] \times 100 \tag{8}$$

where I_{corr} and I_{corr}(inh) are the uninhibited and inhibited corrosion current densities, respectively.

Table 6 Thermodynamic functions of activation of the prepared surfactants.

Inhibitor code	Temperature (K)	E_a^* (kJ mol^{-1})	$-\Delta G^*$ (kJ mol^{-1})	ΔH^* (kJ mol^{-1})	ΔS^* (kJ mol^{-1} K^{-1})
Blank	303	9.64	−22.00	11.98	0.112
	318		−23.83	12.10	0.113
	328		−24.88	12.19	0.113
	338		−25.78	12.27	0.112
QL1	303	38.06	−16.88	54.597	0.189
	318		−19.31	55.708	0.188
	328		−21.27	56.107	0.189
	338		−24.18	55.553	0.192
QL2	303	26.68	−17.73	53.751	0.154
	318		−20.00	55.017	0.155
	328		−21.29	56.087	0.154
	338		−23.57	56.167	0.156
QL3	303	30.04	−16.54	54.935	0.162
	318		−18.66	56.357	0.161
	328		−21.02	56.359	0.163
	338		−22.36	57.38	0.163
QL4	303	28.68	−16.85	54.632	0.158
	318		−19.69	55.325	0.160
	328		−21.36	56.019	0.160
	338		−22.57	57.169	0.159
QL5	303	33.43	−16.67	54.812	0.173
	318		−18.66	56.36	0.172
	328		−21.12	56.261	0.174
	338		−23.06	56.675	0.175
QP1	303	44.63	−15.50	55.984	0.206
	318		−19.25	55.77	0.209
	328		−21.63	55.748	0.210
	338		−23.14	56.6	0.208
QP2	303	60.54	−13.40	58.08	0.252
	318		−17.87	57.146	0.254
	328		−21.76	55.613	0.259
	338		−22.55	57.188	0.254
QP3	303	68.77	−13.41	58.064	0.279
	318		−20.10	54.915	0.287
	328		−22.19	55.183	0.285
	338		−24.11	55.624	0.283
QP4	303	36.17	−16.47	55.006	0.182
	318		−19.72	55.3	0.184
	328		−21.42	55.962	0.183
	338		−23.27	56.462	0.184
QP5	303	47.68	−14.05	57.428	0.212
	318		−17.93	57.085	0.214
	328		−20.14	57.238	0.215
	338		−22.04	57.697	0.214

Table 7 indicates that, the surfactant inhibitor has the ability to inhibit both anodic and cathodic reactions because $\Delta E_{corr} \approx 5$–30 mV. So it was a mixed inhibitor [38]. This means that the inhibitor has a significant effect on retarding the cathodic hydrogen evolution reaction and inhibiting the anodic dissolution of carbon steel.

This behavior supports the adsorption of inhibitor onto metal surface and caused a barrier effect for mass and charge transfer for anodic and cathodic reactions [39].

Lower corrosion current densities (I_{corr}) were observed with increasing the concentration of the inhibitor with respect to the blank inhibitor free solution. This because the effect of the inhibitor was to displace current density to lower values (lower corrosion rate). This behavior confirms a greater increase in the energy barrier of carbon steel dissolution process [29] relative ability of a material to resist corrosion. Since R_p was inversely proportional to I_{corr}, the materials with the highest R_p (and thus the lowest I_{corr}) have the highest corrosion resistance [40].

The value of inhibition efficiency was increased with increasing the inhibitor concentration, Table 7, indicating that a higher surface coverage was obtained in 1 M HCl with the optimum concentration of the inhibitor. This could be

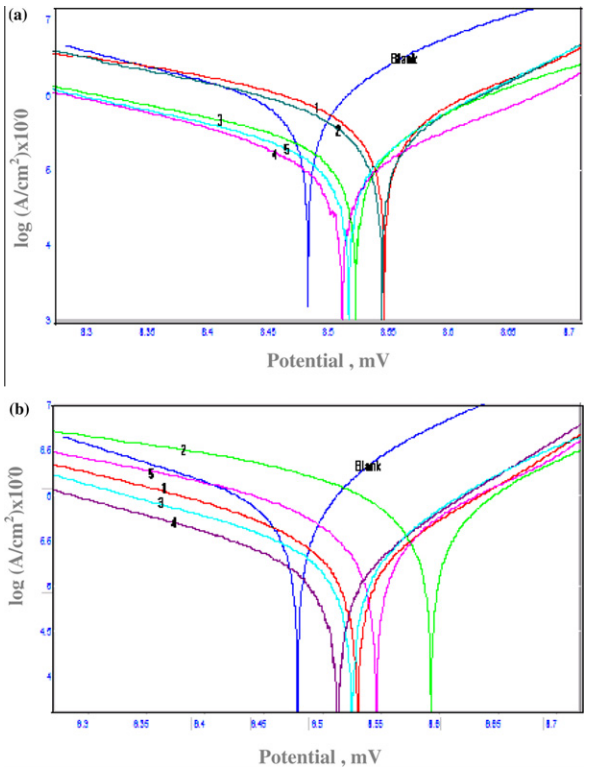

Figure 6 Potentiodynamic polarization curves of carbon steel in 1 M HCl in Absence and presence of 200 ppm of Inhibitor (a) QL_n and (b) QP_n at 303 K.

Table 7 Data from potentiodynamic polarization of carbon steel in 1 M HCl containing 200 ppm of inhibitors at 298 K.

Inhibitor	$-E_{corr}$ (mV)	I_{corr} (mA/cm^2)	R_p (Ohm cm^{-2})	(θ)	E.I. (%)
Blank	521	0.7023	42.29	–	–
QL1	457.3	0.221	101.43	0.685	68.53
QL2	459.4	0.243	101.43	0.685	65.39
QL3	479.9	0.199	222.53	0.716	71.65
QL4	487.4	0.143	56.98	0.798	79.89
QL5	498.7	0.141	87.76	0.798	79.89
QP1	512.6	0.194	267.3	0.808	80.89
QP2	494.8	0.165	76.85	0.764	76.47
QP3	492.4	0.156	98.93	0.777	77.73
QP4	520.9	0.186	85.98	0.734	73.44
QP5	481.4	0.137	222.53	0.804	80.40

explained on the basis of inhibitor adsorption on the metal surface and the adsorption process enhances with increasing inhibitor concentration [41].

The values of cathodic Tafel slope (bc) and anodic Tafel slope (ba) of surfactants were found to change with inhibitor concentration, indicates that the inhibitors controlled both the reactions [42]. In other words, the inhibitors decrease the surface area for corrosion without affecting the mechanism of corrosion and only cause inactivation of a part of the surface with respect to the corrosive medium.

The inhibition efficiency (I.E.%) values obtained from the weight loss measurements were slightly higher than those obtained by electrochemical techniques. The difference may be attributed to the fact that, the weight loss method gives average corrosion rates, whereas the electrochemical method gives instantaneous rates because they were recorded at a much shorter time interval and reflect the corrosion behavior at the initial stage. On the other hand, the high I.E.% values were found such that they indicate a strong adsorption favored by the long duration of the experiments. Therefore, the weight loss experiments confirmed the electrochemical results regarding the adsorption of inhibitors on the carbon steel surface forming a protective film barrier. However, the results obtained from weight loss and potentiodynamic polarization were in reasonably good agreement.

3.8. Quantum chemical calculations

To investigate the relationship between molecular structure of these QASs and their inhibition effect, quantum chemical calculations were performed. Geometric structures and electronic properties of QL1,4,5 and QP3,4,5 as representative samples used as corrosion inhibitors were calculated by ab initio method with 3-21G** basis set. The optimized molecular structures and the frontier molecule orbital density distribution of the studied molecules are shown in Fig. 7. Charge density distribution are given in Table 8. Calculated quantum chemical indices EHOMO, ELUMO, ΔE, dipole moment are given in Table 9. For HOMO (see Fig. 7) of the studied compounds, it can be observed that the increase in bond length makes distortion motion in the solution which increase the $\Delta G_{\text{free energy}}$. For QL1 and QP3 (C12/C12,C16/C16) the geometric structure of this inhibitor is tri angle look like structure which make good I.E. while the geometric structure of QL4 and QP4 make head and tail look like structure which are the lowest I.E. It can be observed that for QL5 and QP5 (built on aromatic 3° amine) the benzene ring, –C═N– has larger electric density coming from the pz orbital of π bond. Low values of the dipole moment will favor the accumulation of inhibitor molecules on the metallic surface. The lowest value of dipole moment was obtained by QL1 (7.42) and QP3 (5.21). These inhibitors exhibit the maximum inhibition efficiency (see Table 1). The bond angle (C–N–C) was found equal in all quantum calculated compounds equal 109.47°, also bond length equal 1.52 Å in all calculated compounds.

The HOMO–LUMO gap, i.e., the difference in energy between the HOMO and LUMO, is an important stability index [43]. We can mention the energy of the HOMO, which is often associated with the capacity of a molecule to donate electrons. Therefore, an increase in the values of HOMO can facilitate the adsorption and therefore the inhibition efficiency, by indicating the disposition of the molecule to donate orbital electrons to an appropriate acceptor with empty molecular orbitals. In the same way low values of the energy gap ΔE = EHOMO – ELUMO will render good inhibition efficiencies, because the energy needed to remove an electron from the last occupied orbital will be low [44,45]. It has been reported in the literature that the higher the HOMO energy of the inhibitor, the greater the trend of offering electrons to unoccupied d orbital of the metal, and the higher the corrosion inhibition efficiency. In addition, the lower the LUMO energy, the easier the acceptance of electrons from metal surface, as the LUMO–HOMO energy gap decreased and the efficiency of inhibitor improved. The data of HOMO and LUMO for our inhibitors are listed in Table 9. Regarding from ΔE it was

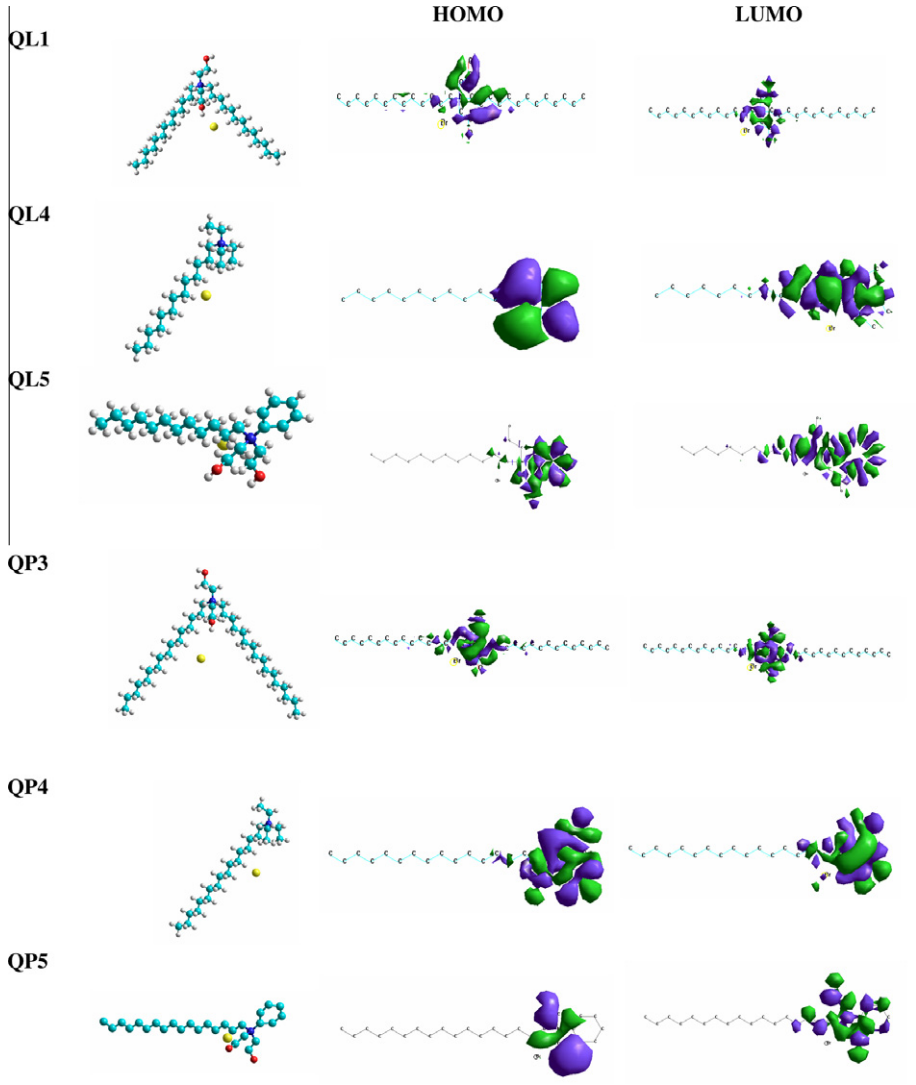

Figure 7 Molecular structure and HOMO–LUMO of QL_n and QP_n.

Table 8 Charge distribution of the studied inhibitors.

Bond	QHL1	QHL4	QHL5	QHP3	QHP4	QHP5
Charge distribution	N = −1.46 O31 = −0.14 O33 = −0.50	N = −1.33 C20 = −0.17 Br = 1.93	N = −1.56 O25 = −0.46 O22 = −0.48 C2 = −0.43 C19 = −0.51	N = −1.62 O7 = −0.42 O9 = −0.51	N = −1.39 C9 = −0.16 Br = 1.87	N = −1.65 O11 = −0.44 O14 = −0.55 C2 = −0.59 C4 = −0.49

Table 9 Calculated quantum chemical parameters of studied inhibitors.

Compound	HOMO (eV)	LUMO (eV)	HOMO–LUMO (eV) ΔE	Dipole moment (u)
QHL1	−47.77	33.51	−81.28	11.52
QHL4	−49.37	35.57	−84.94	16.85
QHL5	−55.76	15.85	−71.61	7.42
QHP3	−52.31	21.74	−74.05	10.75
QHP4	−50.66	41.25	−91.91	14.72
QHP5	−48.14	12.57	−60.71	5.21

found that the minimum value obtained by QL5 and QP5 which have the best inhibition efficiency.

4. Conclusion

The conclusion of this work can be stated in the following points:

1. The maximum inhibition efficiency 96.32% exhibited by QP1, which based on aliphatic tertiary amine (the alkyl halide chain = 16C and the 3° aliphatic amine chain = 16C), meanwhile the QP5 which based on aromatic 3° amine exhibited 98.31% (The alkyl halide chain = 16C and the aromatic 3° amine chain = phenyl group). These data means that the shape and the length of the alkyl chain of the tertiary amines plays an important role in the corrosion inhibition efficiency.
2. The optimum alkyl chain length of the alkyl halide is 16C to get the quaternary ammonium salts, have a good inhibition efficiency (C12 = 92%, C14 = 93%, C16 = 98%, C18 = 95%).
3. The potentiodynamic polarization curves indicated that the inhibitors inhibit both anodic metal dissolution and cathodic hydrogen evolution reactions and acted as mixed type inhibitors in 1 M HCl solution.
4. The adsorption of the inhibitors molecules on the metal surface from 1 M HCl solution obeys Langmuir's adsorption isotherm.
5. From the obtained date of weight loss, potentiodynamic polarization and calculated E_a, it can be concluded that these inhibitors act as physicochemical adsorption.
6. The data obtained from quantum chemical calculations give good evidence on the obtained results by weight loss and potentiodynamic polarization technique.

References

[1] G. Trabanelli, Corrosion 47 (1991) 410.
[2] H. Shokry, M. Yuasa, I. Sekine, R.M. Issa, H.Y. El-Baradie, G.K. Gomma, Corros. Sci. 40 (1998) 2173.
[3] B. Sanyal, Prog. Org. Coat. 9 (1981) 165–236.
[4] A. Lgamri, H.A. El Makarimb, A. Guenbour, Prog. Org. Coat. 48 (2003) 63–70.
[5] F. Bentiss, M. Traisnel, N. Chaibi, et al., Corros. Sci. 44 (2002) 2271–2289.
[6] A. Popova, M. Christov, S. Raicheva, et al., Corros. Sci. 46 (2004) 1333–1350.
[7] M.A. Quraishi, H.K. Sharma, Mater. Chem. Phys. 78 (2002) 18–21.
[8] D. Chebabe, Z.A. Chikh, N. Hajjaji, et al., Corros. Sci. 45 (2003) 309–320.
[9] E. Elayyachy, A. El Idrissi, B. Hammouti, Corros. Sci. 48 (2006) 2470–2479.
[10] M.A. Migahed, A.A. El-Safei, A.S. Fouda, M.A. Morsi, Egypt J. Chem. 45 (2002) 571.
[11] M.A. Migahed, H.M. Mohamed, A.M. Al-Sabagh, Mater. Chem. Phys. 80 (2003) 169.
[12] M.A. Migahed, E.M.S. Azzam, A.M. Al-Sabagh, Mater. Chem. Phys. 85 (2004) 273.
[13] M.A. Migahed, R.O. Alyand, A.M. Al-Sabagh, Corros. Sci. 46 (2004) 253.
[14] M.M. Osman, A.M. Omarand, A.M. Al-Sabagh, Mater. Chem. Phys. 50 (1997) 271.
[15] M.M. Osman, R.A. El-Ghazawy, A.M. Al-Sabagh, Mater. Chem. Phys. 80 (2003) 55.
[16] Z. Abdel Hamid, T.Y. Soror, H.A. El-Dahan, A.M. Omar, Anti-Corros. Methods Mater. 45 (1998) 306.
[17] G. Latha, S.R. Ajeswari, Anti-Corros. Methods Mater. 43 (1996) 19.
[18] N. Pebere, M. Duprat, F.D. Abosi, A. Lattes, J. Appl. Electrochem. 18 (1988) 225.
[19] M.L. Free, Corros. Sci. 44 (2002) 2865.
[20] D.P. Weinsberg, V.A. Shworth, Corros. Sci. 28 (1988) 539.
[21] Arthur I. Vogel, A Textbook of Practical Organic Chemistry, third ed., Logmans, 1956.
[22] R.M. Marwa, M.Sc. Thesis, Faculty of Science, Al-Azhar Al-Shareif University, 2002..
[23] R.G. Andrew, M.M. Michael, M.P. Rama, J. Dispersion Sci. Technol. 27 (2006) 731.
[24] M.A. Hegazy, Corros. Sci. 51 (2009) 2610–2618.
[25] ASTM, G31, Standard Practice for Laboratory Immersion Testing of Metal, 1972 (Reproved 1990).
[26] G. Avci, Colloids Surf. A Physicochem. Eng. Aspects 317 (2008) 730–736.
[27] A.M. Al-Sabagh, N.M. Nasser, N.Gh. Kandile, M.A. Migahed, J. Dispersion Sci. Technol. 29 (2008) 161.
[28] L.M. Vracar, D.M. Drazic, Corros. Sci. 44 (2002) 1669.
[29] F.K. Kerkouche, A. Benchettara, S. Amara, Mater. Chem. Phys. 110 (2008) 26–33.
[30] M.R. Saleh, A.M.S.E. Din, Corros. Sci. 12 (1981) 688.
[31] A.K. Maayta, N.A.F. Al-Rawashdeh, Corros. Sci. 46 (2004) 1129.
[32] S.K. Shukla, M.A. Quraishi, Corros. Sci. 51 (2009) 1990–1997.
[33] A.M. Badiea, K.N. Mohana, Corros. Sci. 51 (2009) 2231–2241.
[34] S.V. Ramesh, A.V. Adhikari, Mater. Chem. Phys. 115 (2009) 618–627.
[35] M.A. Hegazy, M.F. Zaky, Corros. Sci. 52 (2010) 1333–1341.
[36] M. Behpour, S.M. Ghoreishi, N. Soltani, M. Salavati-Niasari, M. Hamadanian, A. Gandomi, Corros. Sci. 50 (2008) 2172–2181.
[37] R.A. Prabhu, T.V. Venkatesha, A.V. Shanbhag, G.M. Kulkarni, R.G. Kalkahmbkar, Corros. Sci. 50 (2008) 3356–3362.
[38] S.Z. Yao, X.H. Jiang, L.M. Zhou, Y.J. Lv, X.Q. Hu, Mater. Chem. Phys. 104 (2007) 301–305.
[39] M.A. Migahed, M. Abd-El-Raouf, A.M. Al-Sabagh, H.M. Abd-El-Bary, Electrochim. Acta 50 (24) (2005) 4683–4689.
[40] Z. Zhang, S. Chen, Y. Li, S. Li, L. Wang, Corros. Sci. 51 (2009) 291–300.
[41] F.G. Liu, M. Du, J. Zhang, M. Qiu, Corros. Sci. 51 (2009) 102–109.
[42] A.M. Sabagh, N.G. Kandil, A.M. Badawi, H. El-Sharkawy, Colloids Surf. A Physicochem. Eng. Aspects 170 (2000) 127.
[43] D.F.V. Lewis, C. Ioannides, D.V. Parke, Xenobiotica 24 (1994) 401–408.
[44] N. Khalil, Electrochim. Acta 48 (2003) 2635.
[45] P. Molymeux, C.T. Rhodes, J. Swarbrick, Trans. Faraday Soc. 61 (1965) 1043.